



## Prediction of Smear Effect on the Bearing Capacity of Driven Piles

**Dr. Ala'a Hussein. Alwan Al-Zuhairi**  
Lecturer, Eng. College-Civil Dept.  
Baghdad University  
Email: alaalwn@yahoo.com

**Hayder Alwan Mahdi**  
Ass. Lecturer, Eng. College-Civil  
Dept Baghdad University  
Email:civil\_hayder1974@yahoo.com

**Saif Mohammed Jawad**  
Ass. Lecturer,Eng. Dept.  
Baghdad University  
Email:s1981aif@yahoo.com

### Abstract

This paper deals with prediction the effect of soil remoulding (smear) on the ultimate bearing capacity of driven piles. The proposed method based on detecting the decrease in ultimate bearing capacity of the pile shaft (excluding the share of pile tip) after sliding downward. This was done via conducting an experimental study on three installed R.C piles in a sandy clayey silt soil. The piles were installed so that a gap space is left between its tip and the base of borehole. The piles were tested for ultimate bearing capacity according to ASTM D1143 in three stages. Between each two stages the pile was jacked inside the borehole until a sliding of about 200mm is achieved to simulate the soil remoulding due to actual pile driving. The results of the tests exhibited that the pile might loss 14% of its ultimate capacity when it is loaded immediately after installation. Also, it was concluded that the pile may regain of about 9% of its original capacity after 30days of its installation.

**Key words:** Driven piles, bearing capacity, smear, soil remoulding, pile testing.

( )

ASTM D1143

( )

200 ( )

( )

%9

%14

30

## 1. Introduction

Piles are structural members usually used to transfer the bearing loads coming from structure they support to the deeper strong strata. According to the method of their installation, piles can be divided into two groups:

- (a) Displacement piles, and
- (b) Non displacement piles

Driven piles and preformed-cast in place piles are examples of displacement piles. Driven piles may be of a solid section made of timber, steel or concrete or hollow steel section. The second type of displacement piles (driven cast-in place piles) is formed by driving a close-ended tube into the ground then it is filled with concrete. Non displacement pile is created when a void is formed into the ground by boring or excavation then the void is filled with concrete.

The method of pile installation may have profound effects on its behavior under load (Polous and Davis). It is easy to recognize that these effects are mostly related with displacement piles since the method of their installation generally creates more disturbance than other methods.

### 1.1 Effect of Type of the Soil

On the other hand, the type of surrounding soil has a role in magnification or minimization of the installation effects on pile performance.

#### (a) In clays:

de Mello (1969) classified the effects of pile driving in clays into three classes:

1. Remoulding (smear) of soil particle structure closed to the pile shaft.
2. The stress state of the soil is changed after pile driving due to soil densification i.e. increasing the horizontal stress.
3. Developing of the excess pore pressure then dissipation with time.

Lee et al. (2003) concluded that the state of the soil (density and stress state) is changed significantly when a pile is driven into the ground. D. Basu et al. (2005) noticed that pile driving preloads the surrounding soil, resulting in a greater base resistance than that observed for bored (non-displacement) piles. They found higher ratio of base share of pile capacity to its total capacity ( $q_b/q_c$ ) for displacement piles than that for geometrically

identical non displacement piles ( $q_b$  = capacity of the pile base and  $q_c$  = total capacity of the pile). As it is seen the capacity of pile shaft is decreased due to effects of pile driving. Generally, it may be expected that pile driving process in clay will cause initially loss in undrained shear strength of clay due to remoulding at constant moisture content (Polous and Davis).

Concerning the pore pressures developed during pile driving, a number of measurements have been made. As stated by (Polous and Davis) a summary of some measurements of the variation with radial distance of the excess pore pressure around a single driven pile are given in Fig. 1. In this figure the normalized excess pore pressure is

indicated  $\frac{\Delta u}{\Delta \sigma'_{vo}}$  where  $\Delta u$  is the excess pore

pressure and  $\Delta \sigma'_{vo}$  is the vertical effective stress in the soil prior to driving. It is seen there is a considerable scatter in the points resulting largely from differences in soil type. The larger pore pressure being associated with the more sensitive soils. However, D'Appolonia and Lambe (1971) derived eq.(1) to estimate the maximum pore pressure developed near the pile surface.

$$\frac{\Delta u}{\Delta \sigma'_{vo}} = \left[ (1 - k_o) + \frac{2S_u}{\sigma'_{vo}} \right] A_f \quad (1)$$

Where,

$\Delta u_m$  = maximum excess pore pressure

$K_o$  = in situ coefficient of earth pressure at rest

$S_u$  = undrained shear strength

$A_f$  = pore pressure coefficient A at failure

$\sigma'_{vo}$  = initial vertical effective stress in soil

#### (b) In sands:

The soil is compacted by displacement and vibration resulting from permanent rearrangement and some crushing of the particles. The pile capacity is increased when the soil is in loose condition due to increase in relative density caused by pile driving. Kishide (1967) proposed a simple method to estimate the effect of driving a pile in loose sand. He assumed that the diameter of the compacted zone around the driven pile is seven



times the pile diameter (d). Also, he assumed that the change in angle of friction  $\phi'$  is linear with the distance from the original value of  $\phi'_i$  at the pile tip as clarified in eq.(2) (see Fig. 2):

$$\phi'_2 = \frac{\phi'_i + 40}{2} \quad (2)$$

From eq.(2) it is concluded that when  $\phi'_i = 40^\circ$ , which is the case of dense sand, there is no change in relative density due to pile driving.

Paik and Salgado (2004) investigated the effect of pile installation method on pipe pile behavior (penetration parameters and bearing capacity) in sands via calibration chamber test conducted on model pipe piles installed in different sandy soil conditions. They concluded that the pile capacity is increased with increasing hammer weight at the same driving energy and with increasing hammer weight at the same fall height. Finally, they observed that the jacked piles have higher bearing capacities than identical driven piles under similar conditions.

**2. Experimental Works**

To performer the goal of this study, an experimental program is conducted on two stages:

**2.1 Laboratory Stage**

In this stage routine classification tests were conducted on disturbed samples taken from three boreholes prepared for piles. The tests consist of specific gravity, Aterberg limits and grain size distribution. The results of some of these tests are listed in Table 1 and others are shown in Fig. 3. Although soil samples were extracted from different depths, the results of the tests showed almost the same physical properties. Moisture content, unit weight and unconfined compression tests were excuted on undisturbed samples taken from the three drilled boreholes. The results of these tests were tabulated in Table 1.

The aggergates prepared for concrete piles (sand and gravel) were also tested for gradation and undesirable matter content according to Iraqi Standard (IQS 45:1984). The sulphate resistance cement is tested for physical properties according to (IQS 5:1984). A concrete mix was designed to achieve 28-days compressive strength of 30MPa following the proceduer given by ACI 211.1-91. The results of tests and mix proportions are listed in Table 2.

**Table 1: Physical and Mechanical properties of the ground soil**

Property	Depth of sample (m)	Borhole(1)	Borhole(2)	Borhole(3)
Specific Gravity, G <sub>s</sub>	0.75	2.67	2.71	2.72
	1.75	2.76	2.74	2.80
	2.75	2.75	2.73	2.78
Liquid limit, L.L (%)	0.75	33.2	32.7	31.4
	1.75	35.5	38.0	34.8
	2.75	38.8	37.8	39.2
Plasticity index, P.I (%)	0.75	12.0	11.8	12.2
	1.75	13.6	14.1	13.0
	2.75	14.5	15.8	14.2
Moisture content, w <sub>c</sub> (%)	1.0	16.2	15.8	16.3
	2.0	17.0	17.2	16.8
	3.0	17.2	17.4	17.4
Dry Unit weight, $\gamma_d$ (kN/m <sup>3</sup> )	1.0	16.88	16.74	16.26
	2.0	17.01	16.92	16.85
	3.0	16.98	16.84	16.91
Unconfined compression, q <sub>u</sub> (kPa)	1.0	78.1	79.1	77.4
	2.0	112.6	108.4	112.0
	3.0	118.7	116.8	117.1

## 2.2 Field Stage

### Pile installation

Three 150mm diameter boreholes were drilled to a depth of 3m below ground level in the University of Baghdad near Al-Khawarizmi Engineering College at Al-Jadiriah using the hand auger. No water table was distinguished in all boreholes. To make side skin friction of pile is the only active component of the pile capacity (i.e. to vanish the tip component of the bearing capacity) during pile loading, a gap is left between concrete pile tip and the end of boring. This was made by utilizing a circular steel plug plate fixed at the bottom of reinforcement cage of the pile as shown in Fig. 4. The reinforcement cages were placed in the boreholes so that the piles are installed leaving a gap distance of 500mm between pile tip and borehole base. Then the concrete is poured inside the holes with light compaction to the final top level which is achieved by using a PVC pipe mould as shown in Fig. 5.

### Pile testing

After casting, the piles are left for thirty days to permit for concrete maturation. Then each of the three installed piles are subjected to the following procedure of loading and unloading using a hydraulic jack of 35ton capacity, 0.01mm dial gage, reference beam and steel pipe of closed ends as a loading column. The cantilever beams of neighbor building are employed as reaction beams

during pile testing. The details of the loading apparatus are shown in Fig. 6:

1. The pile was loaded according to the method described in ASTM D1143. The theoretical estimated maximum bearing load of the pile was incremented into four equal 25% increments. In each increment, the applied load is maintained by continuously jack force increasing until the rate of settlement that specified in ASTM D1143 (0.25mm/hr) is reached. Incremental loading was continued by jacking the pile until a settlement of about 15% of the pile diameter is obtained or when the pile can not carry any additional load whichever is nearest. In the present work all piles failed by the former criterion. Then the load is removed in decrements of 25% of the total load with one hour between decrements and settlement recovery of the pile is recorded.
2. After this stage of testing, the pile is driven to about 200mm inside the borehole by rapid continuous jacking on its head. This stage simulates the effects of particles remoulding (smear) of the surrounding soil during pile driving.
3. The piles are left for 0, 10 and 30days before the next cycle of loading is resumed.
4. The second cycle is conducted following steps (1), (2) and (3) mentioned above.
5. The last cycle is done following the same instructions of step (1).

The results of the test of the three piles can be seen in Figs. 7.

**Table 2: Material properties and concrete mix proportions**

	Cement		Water	Fine agg. (sand)		Coarse agg. (gravel)	
	Property	Results		Seive size (mm)	Passing by weight (%)	Seive size (mm)	Passing by weight (%)
Material Properties	Initial setting time (min)		56	10	100	37.5	100
	Final setting time (hr)		3.5	4.75	92.0	20	98.5
	Compressive strength (MPa)	3 days	18.2	2.36	75.6	10	41.4
		7 days	24.1	1.18	53.2	5	0.9
	Fineness (m <sup>2</sup> /kg)		273	0.6	33.0		
				0.3	17.6		
				0.15	8.2		
				SO <sub>3</sub> (%)	0.23	SO <sub>3</sub> (%)	0.067
				Fines (%)	4.7	Fines (%)	0.2
	Final result	Pass		Pass (Zone 2)		Pass (grade 20-5)	
Conc. mix proportions	1		0.487	1.632		2.241	



### 3. Results and Discussion

Fig. 7 shows the load-settlement curves for the tested piles in three cycles of loading. The curves of the first cycle for all three piles exhibit almost the same trend since the piles are distributed in rather small area of ground, the case in which the same condition of soil is predominated as it was clarified in Table 1. Generally, the curves exhibit a decrease in ultimate pile capacity at second and third cycles for a given settlement. This is attributed to the decrease in shear strength of the surrounding soil due to particle remoulding (smear) that caused capacity. This finding comes compatible with the observation of Polous and Davis (1980). They described the regain with time of lost shear strength of the surrounding soil due to pile driving as a thixotropic regain of undrained strength as the structural bonds destroyed by remoulding are at least partially restored.

To study the effect of surrounding soil remoulding (i.e. smear) caused by shaft sliding on pile bearing capacity, the maximum measured pile capacity in each cycle of each pile were plotted against the number of cycle in Fig. 8. The calculated theoretical average maximum pile capacity was also indicated on the same figure. The curves indicate a decrease in maximum pile capacity in a range of (1.9-6.3)kN which represent a (4.3-14)% of the theoretical average maximum capacity. The effect of time lag between loading cycles (smear aging) on the regain of destroyed adhesion between pile shaft and surrounding soil is clarified in Fig.9. The piles regained (2.5-4.6)% after 10days and (3.5-9.4)% after 30days of the original measured ultimate pile capacity.

### 4. Conclusions

From the results of the experimental work that executed during this study, the following conclusions can be drawn:

1. The proposed new method is based on destroying the adhesion bond between pile shaft and surrounding soil by sliding the pile shaft without tip resistance after installation to simulate the effect of soil remoulding due to actual pile driving.
2. 14% of the ultimate pile capacity may be lost when it is loaded immediately after installation while only 4.6% may be lost when the pile loaded after 30days.

by driving of the pile shaft. The decrease in shear strength of a soil when its particles remoulded is referred to sensitivity which is a property of the cohesive soils. In this study, the tested soil was found generally plastic silt (see Fig. 3). The plasticity came from the ability of the soil to absorb water and transfer from plastic to liquid state (i.e. plasticity index) see Table 1. This may stand behind its behavior after remoulding that caused by pile driving. The decrease in pile capacity was found dependent on time lag between cycles. The more the time lag between the cycles the less decrease in pile capacity. When linear variation is assumed for shear strength lossing and regaining during pile driving, the regain of the lost shear strength may be taken equals the regain of measured pile capacity after a certain time period. Consequently, a percentage of (2.5-4.6)% of the original shear strength of the soil is regained after 10days and (3.5-9.4)% after 30days of the pile installation.

### References:

- ACI Committee 211, 2008, "Standard Practice for Selecting Proportions for Normal, Heavyweight, and Mass Concrete." (211.1-91), American Concrete Institute, Detroit.
- ASTM D1143-81 (reapproved 1994), "Standard Test Method for Piles under Static Axial Compressive Load", Annual Book of ASTM Standards, Vol. 04.08, New York, USA.
- Basu, D., Salgado, R., Prezzi, M., Lee, J. and Paik, K., "Recent Advances in the Design of Axially-Loaded Piles in Sandy Soils", 2005, Advances in Deep Foundation, ASCE, (Downloaded from the site [www.ascelibrary.org](http://www.ascelibrary.org)).
- D'Appolonia, D.J. and Lambe, T. W., 1971, "Performance of Four Foundations on End-Bearing Piles", Soil Mechanics and Foundation Engineering Journal, ASCE, Vol. 97 SM10, pp. 77-93.
- de Mello, V.F., 1969, "Foundation of Buildings on Clay.", Proceeding of 7<sup>th</sup> International Conference in Soil Mechanics and Foundation Engineering, Mexico City, pp. 49-136
- Head, K.H., 2006, "Soil Laboratory Testing", Volumes 1, 2 and 3, 3<sup>rd</sup> Edition, Whittles Publishing, Scotland, U.K.

Kishida, H., 1967, "Ultimate Bearing Capacity of Piles Driven into Loose Sand.", Soils and Foundations, Vol.7 No.3,pp. 20-29

Lee, J. H. Salgado, R. and Paik, K. (2003), "Estimation of the Load Capacity of Pipe Pile in Sand Based on Cone Penetration Test Results.", Journal of Geotechnical and Geoenvironmental Engineering., ASCE, Vol. 127 pp. 3-16.

Paik, K. and Salgado, R., "Effect of pile Installation Method on Pipe Pile behavior in Sands", Geotechnical Testing Journal (GTJ), Vol. 27, Issue 1 (January 2004).

Poulos, H.G. and Davis, E.H., "Pile Foundation Analysis and Design.", 1980, Rainbow-Bridge Book Co.

Weltman, A. and Little, J., "A Review of Bearing Pile Types" Directorate of Civil Engineering Services (DOE) and Construction Industry Research and Information (CIRIA) Report PG1, 1977 London.

" (IQS 5:1984)

"

8 1984

" (IQS 45:1984)

"

8 1984

Legend:

- Wallaceburg (Lo and Stermac, 1965)
- △ Ghost River (Lo and Stermac, 1965)
- Wabi River (Lo and Stermac, 1965)–(29 ft depth)
- Wabi Riber (Lo and Stermac, 1965)–(37 ft depth)
- × Marine Clay (Bjerrum and Johannessen, 1960)–(7.5 m depth)
- ▲ Marine Clay (Bjerrum and Johannessen, 1960)–(10 m depth)
- ▽ Firm Clay (Airhart et al., 1969)–(40 ft depth)
- + Boston Blue Clay (D'Appolonia and Lambe, 1970)
- Varved Clay (Soderman and Milligan, 1961)–(20 ft depth)
- ▼ Varved Clay (Soderman and Milligan, 1961)–(25 ft depth)
- ◇ Varved Clay (Soderman and Milligan, 1961)–(30 ft depth).

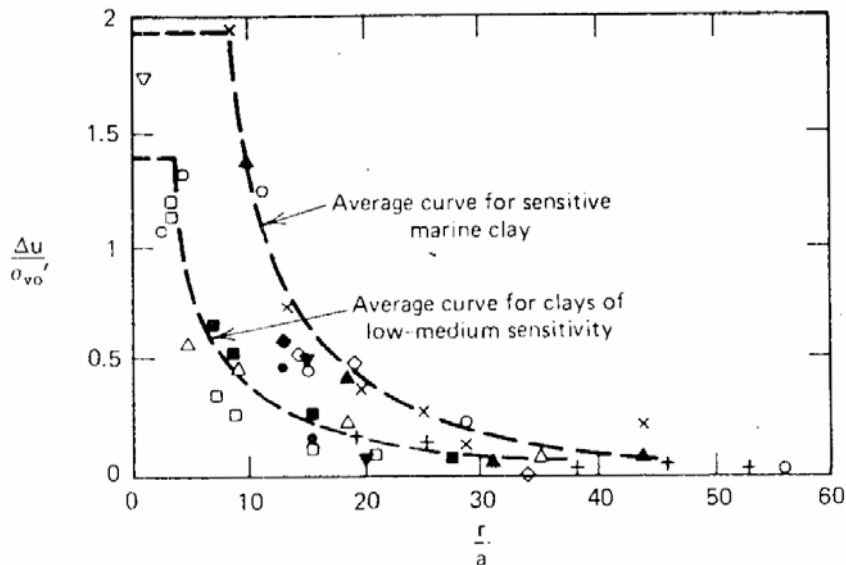


Fig. 1: Summary of measured pore pressures (Polous and Davis, 1980)

Note:  $\frac{r}{a}$  = the ratio between the distance from pile center to point at which the pore is measured to the diameter of the pile

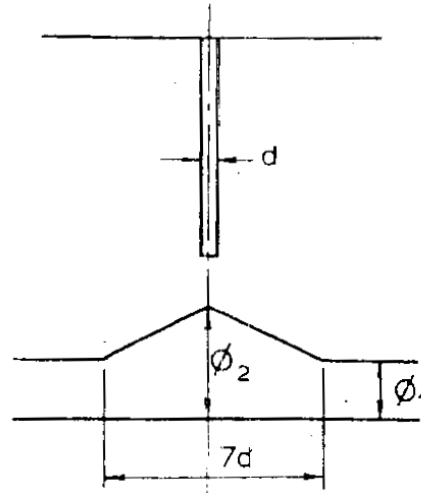


Fig. 2: Effect of pile driving on the angle of internal friction ( $\phi$ ) in sand (Kishida, 1967)

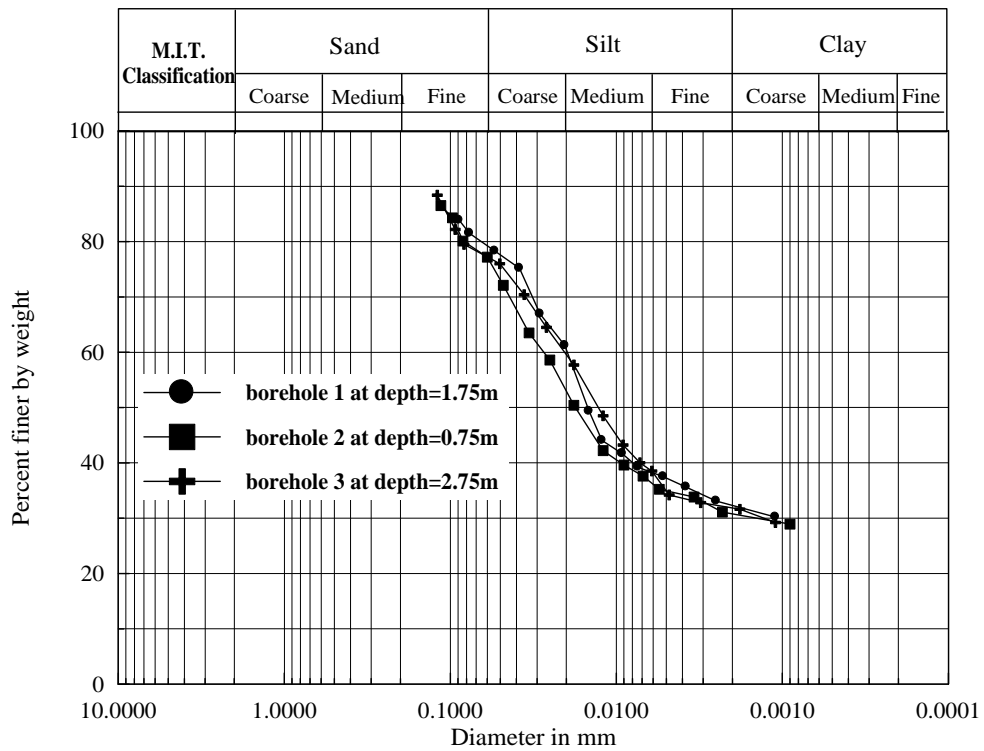


Fig. 3: Grain size distribution of the soil

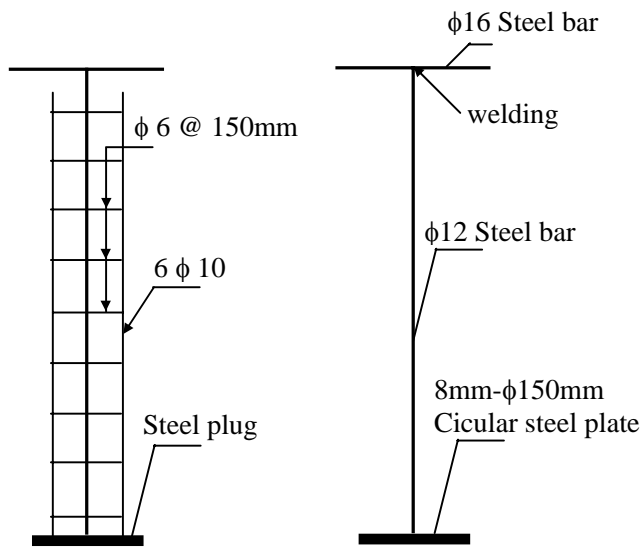


Fig. 4: Pile reinforcement and plug details

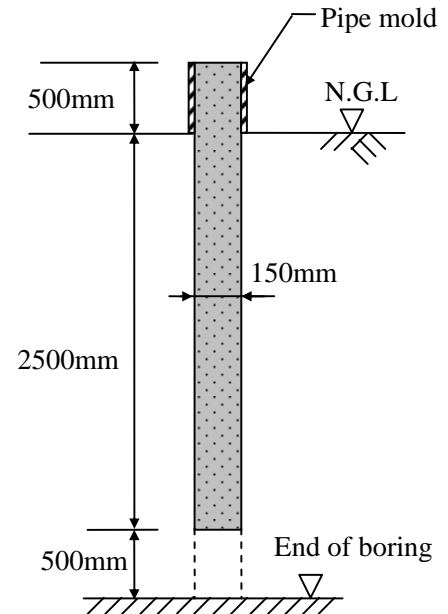


Fig. 5: Pile installation feature

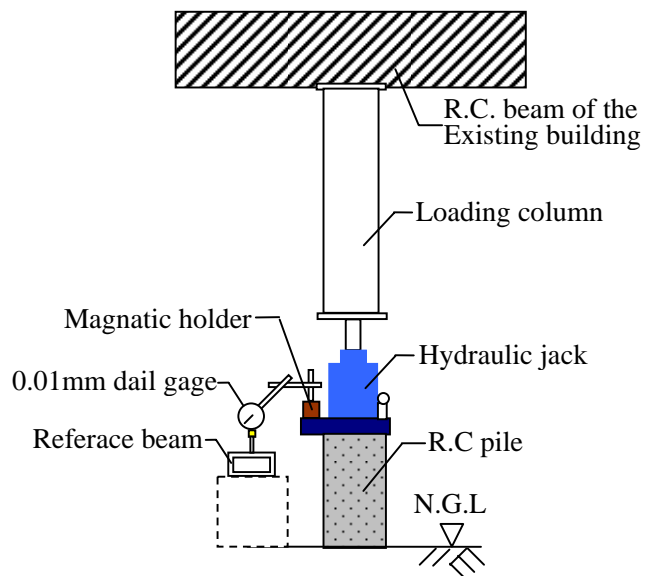
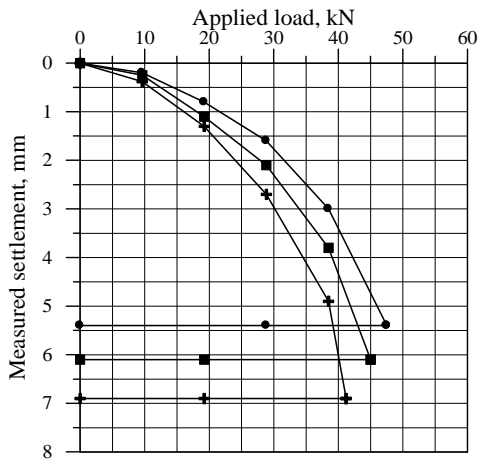
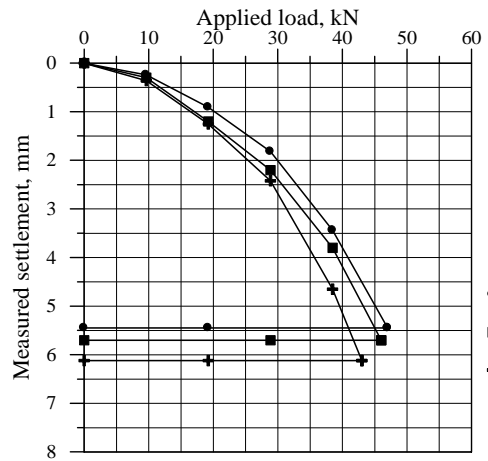


Fig. 6: Loading Apparatus

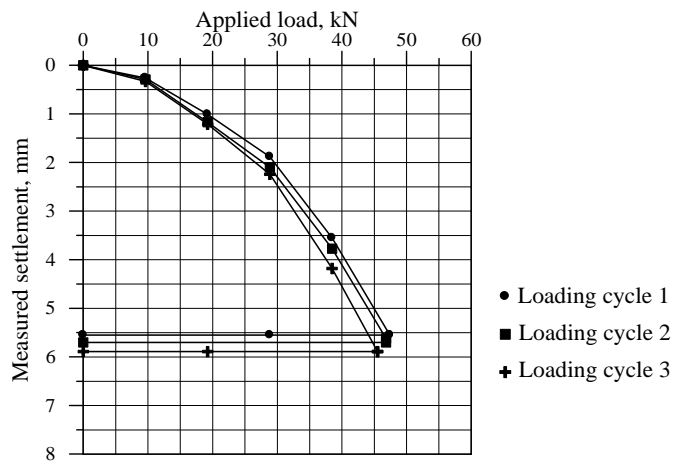




(a) Pile no.(1)



(b) Pile no.(2)



(c) Pile no.(3)

Fig. 7: Load-settlement curves

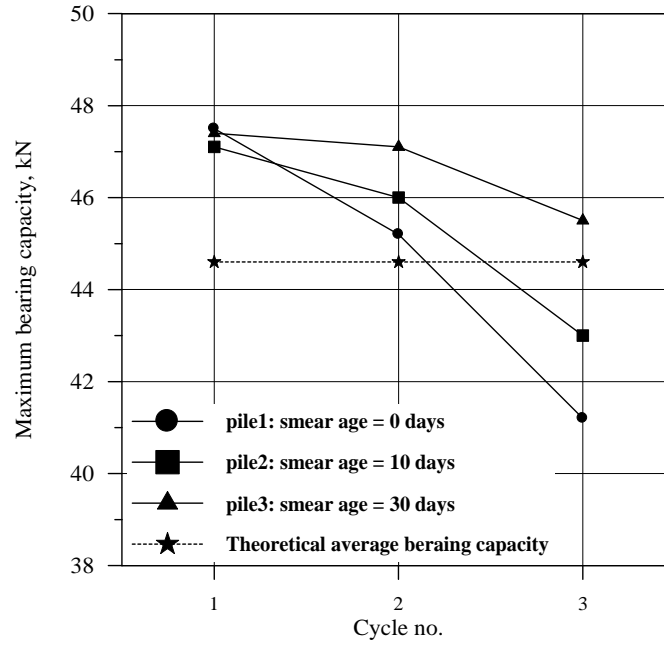


Fig. 8: Maximum measured and theoretical bearing capacities of the piles

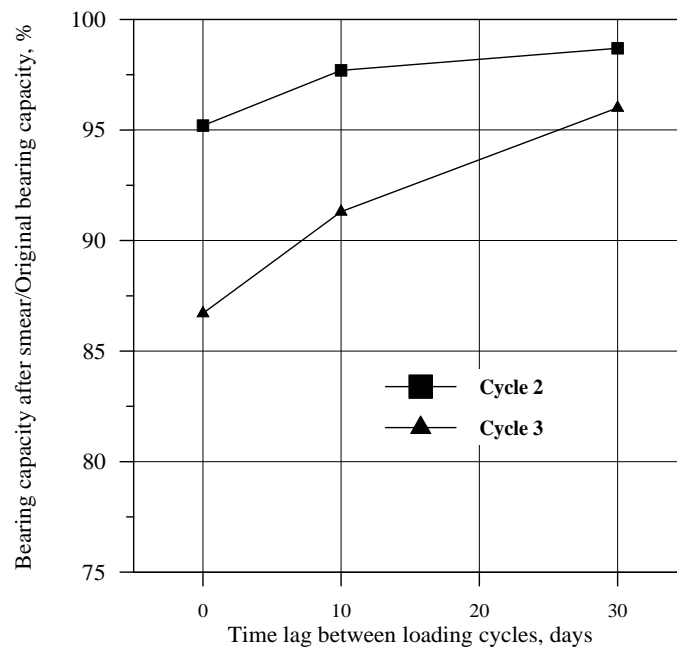


Fig. 9: Effect of smear aging on pile capacity restoring